

## Generalized scale invariance and differential rotation in cloud radiances

S. Lovejoy, D. Schertzer<sup>1</sup> and K. Pflug

*Department of Physics, McGill University, 3600 University St., Montréal,  
Québec H3A 2T8, Canada*

Scale invariant symmetries are usually restricted to systems involving extremely special types of scale changes; self-similar and self-affine fractals involving isotropy and differential stratification respectively. In contrast, geophysical and astrophysical systems can be scale invariant but display complex anisotropy including differential rotation. The formalism required to handle such symmetries is generalized scale invariance; using the new Monte Carlo differential rotation technique we test it on satellite cloud radiances over the range 1–1200 km. Our results underscore the limited usefulness of self-similar and self-affine scaling ideas in atmospheric dynamics since we find substantial differential rotation which is, nevertheless, scaling.

Scale invariance is a symmetry principle in which the small and large scales are related by a scale changing operation which depends only on the scale ratios; there is no characteristic size. Up until recently, almost all attention has been focused on extremely simple types of scale changes [1], primarily ordinary “zooms” (magnifications) associated with self-similar (or asymptotically self-similar) fractals and multifractals. Practically the only other scale changing operation to receive attention by physicists are self-affine transformations in which the zoom is followed by differential “squashing” along coordinate axes.

In contrast, geophysical [2] and astrophysical [3] systems can be scale invariant<sup>#1</sup> but are highly anisotropic; in addition to differential stratification, they often involve differential rotation and other more complex scale changing operations that can vary from place to place even randomly. The need to deal with scale invariant anisotropy has led to the development of the formalism of generalized scale invariance (GSI) [2, 5–7]. The implications of GSI for atmospheric dynamics are particularly exciting since it holds the promise of unifying large and small scale motions. The latter are still widely regarded as being separate isotropic self-similar two- and three-dimensional turbulent regimes respectively.

<sup>1</sup> EERM/CRMD, Météorologie Nationale, 2 Ave. Rapp, 75007 Paris, France.

<sup>#1</sup> A recent preprint [4] develops in the context of Newtonian space/time, a formalism not unlike GSI.

GSI has the following basic ingredients:

(i) A unit “ball”  $B_1$ , which defines all the unit vectors. If an isotropic unit ball exists, we call the corresponding scale the “sphero-scale”.

(ii) A (semi) group of scale changing operators  $T_\lambda = \lambda^{-G}$ , which reduces the scale of vectors by scale ratio  $\lambda$ :  $B_\lambda = T_\lambda(B_1)$  is the ball of all vectors at scale  $\lambda$ . Virtually the only other restriction on  $T_\lambda$  is that the  $B_\lambda$  are strictly decreasing ( $B_\lambda \supset B_{\lambda'}$ ;  $\lambda < \lambda'$ ), hence that the real parts of the (generalized) eigenspectrum [5] of  $G$  are all  $>0$ .

(iii) A measure of scale such as some power of the volume of  $B_\lambda$ ; the exact definition is somewhat a matter of convenience or convention [5]; although the most obvious is to use the fact that if  $\phi^D$  indicates the ordinary volume operator in a space dimension  $D$ , and  $d_{el} = \text{Tr } G$ , then a convenient “elliptical” scale  $\phi_{el}$  is given by the following relation:

$$\phi_{el}^{del}(B_\lambda) = \phi^D(B_\lambda) = \lambda^{del} \phi^D(B_1) = \lambda^{del} \phi_{el}^{del}(B_1) = \lambda^{del}. \quad (1)$$

Note that in GSI size is a measure (not metric) quantity and the type of scale invariance is not specified, i.e. GSI can apply to fractal sets, multifractal measures or other types of scale invariant systems. When  $G$  is a matrix we have “linear GSI”, the anisotropy is position independent. Linear GSI can always be regarded as a local approximation to the full (nonlinear) GSI; it is equivalent to using tangent spaces. When the matrix is the identity, we have self-similar scale invariance; when  $G$  is a diagonal matrix, we have a “self-affine” system; and when off-diagonal elements are present, we have differential rotation. In all cases,  $d_{el}$  is an important characteristic since it quantifies the overall rate of change of volumes of structures.

Up until now, methods for empirically evaluating  $G$  have been limited to estimates of  $d_{el}$ . For example, for atmospheric motions, we [2] obtained  $d_{el} = \frac{23}{9} = 2.555\dots$  in  $(x, y, z)$  space, and for rain [8]  $d_{el} = 2.22 \pm 0.07$ , and also for rain, for space time transformations [9]  $((x, y, t)$  space),  $2.5 \pm 0.3$ . In each case,  $d_{el}$  characterizes stratification,  $d_{el} = 3$  corresponding to isotropic (self-similar) scaling,  $d_{el} = 2$  to complete stratification into horizontal layers. In this note, we report on results of a new “Monte Carlo differential rotation” technique which for the first time enables us to empirically estimate the off-diagonal elements of linear GSI.

We illustrate the method on visible and infra red satellite pictures at 1.1 km resolution <sup>#2</sup> (fig. 1a, b, c). We assume statistical translational invariance of the

<sup>#2</sup> These pictures are from the NOAA 9 satellite and were remapped on regular  $256 \times 256$  and  $512 \times 512$  point grids before the analysis was performed. Details of this and the analysis techniques may be found in ref. [10].

radiance fields; in Fourier space, this implies random phases, hence we examine the modulus of the Fourier amplitudes squared (the spectral energy density, denoted  $P(\mathbf{k})$  at wavenumber  $\mathbf{k}$ , see fig. 2a, b, c). If  $\mathbf{x}_\lambda = T_\lambda \mathbf{x}_1$ , then the corresponding Fourier relation [7]  $\mathbf{k}_\lambda = \tilde{T}_\lambda \mathbf{k}_1$ , where the Fourier operator  $\tilde{T}_\lambda$  has generator  $\tilde{G} = G^T$  (where ‘‘T’’ indicates ‘‘transpose’’). Furthermore, using a decomposition into quaternions (or equivalently into Pauli matrices), we can obtain the following explicit formula for linear GSI in two dimensions:

$$G = \begin{pmatrix} d + c & f - e \\ f + e & d - c \end{pmatrix}, \quad \tilde{G} = \begin{pmatrix} d + c & f + e \\ f - e & d - c \end{pmatrix}, \quad (2)$$

$$\tilde{T}_\lambda = \lambda^{\tilde{G}} = \lambda^d \left( \mathbb{1} \cosh(au) + (\tilde{G} - d\mathbb{1}) \frac{\sinh(au)}{a} \right),$$

$$a^2 = c^2 + d^2 - e^2, \quad u = \log \lambda \quad (3)$$

( $\mathbb{1}$  is the identity matrix). When  $a$  is real, stratification dominates, whereas when  $a$  is imaginary, rotation dominates; these two qualitatively different behaviors have been proposed as a basis for classifying galaxies into barred or spiral types [3].

If  $T_\lambda$  is the real space scale changing operator for second order moments<sup>#3</sup> (structure functions), then the corresponding Fourier space operator satisfies

$$P(\tilde{T}_\lambda \mathbf{k}) = \lambda^{-s} P(\mathbf{k}), \quad (4)$$

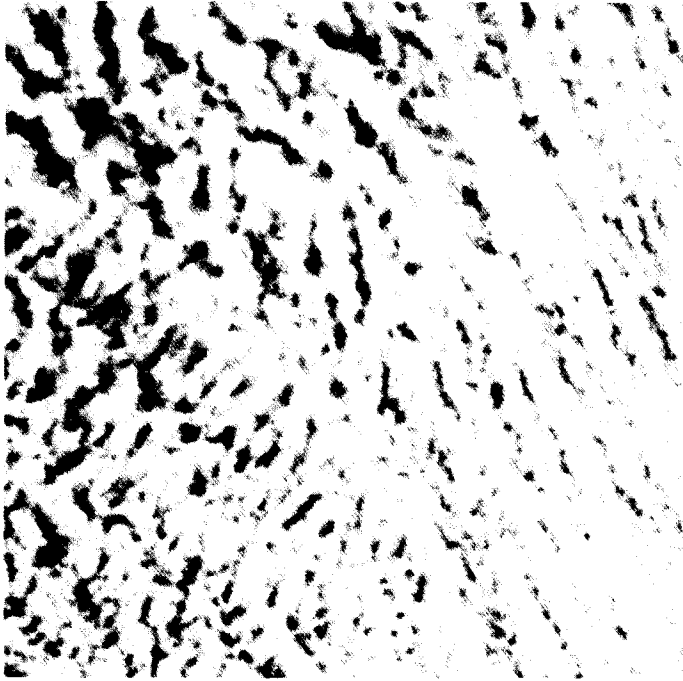
where  $s$  is an (anisotropic) spectral exponent. Hence in fig. 2,  $\tilde{T}_\lambda$  will map one set of isolines of  $P$  onto another.

Unlike the vertical or time axes, which are stratified with respect to the horizontal, the two horizontal directions display no obvious overall stratification; we therefore took our definition of size to be the square root of the area of the  $B_\lambda$ , hence  $d_{el} = 2$ ,  $d = 1$ . To test linear approximations to GSI, we therefore seek to determine  $c, e, f, s$ , the energy density of the unit ball, as well as the shape of the unit ball. In the simplest cases (see fig. 2a, b), a nearly circular ‘‘sphero-scale’’ seems to exist, hence we only require an estimate of the corresponding radius (a total of six parameters). In fig. 2c however, no sphero-scale is apparent; indeed, given the roughly log spiral shape of the cyclone, one does not expect one to exist. In the latter case, we used the following parametrization<sup>#4</sup>:

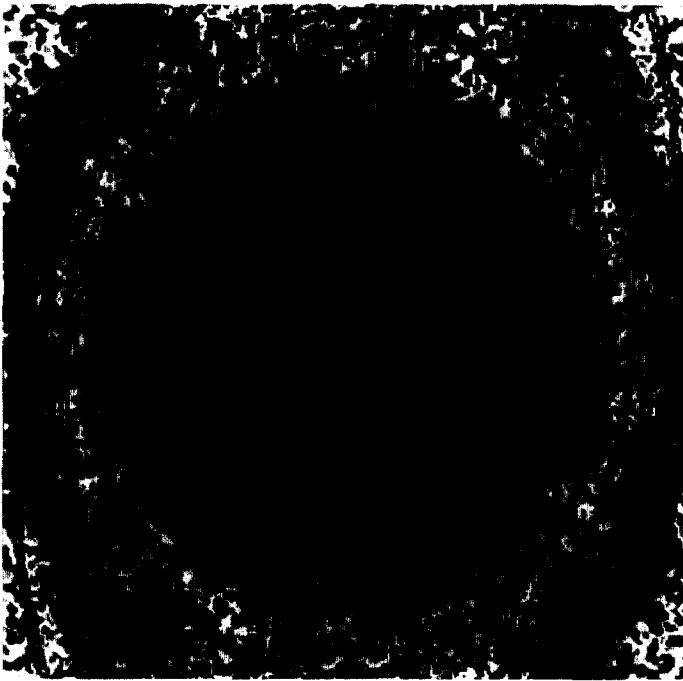
$$r(\theta) = r_0 + a_1 \cos(2\theta) + b_1 \sin(2\theta) + a_2 \cos(4\theta) + b_2 \sin(4\theta). \quad (5)$$

<sup>#3</sup> Since the radiance fields are multifractal [11, 9, 12], we expect the operator to depend on the order of singularity, and hence on the order of statistical moments.

<sup>#4</sup> This polar coordinate parametrization of the unit ball is the first few terms in a Fourier series respecting the Fourier symmetry  $P(\mathbf{k}) = P(-\mathbf{k})$ .

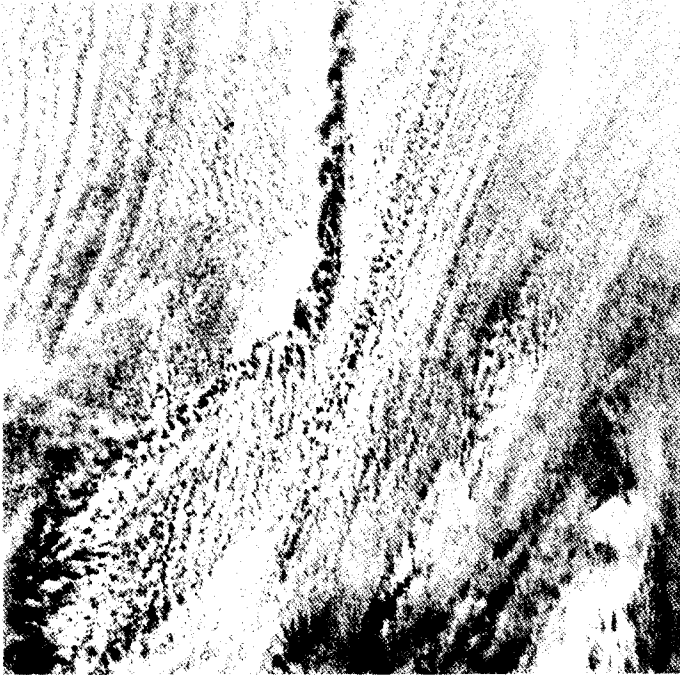


1a

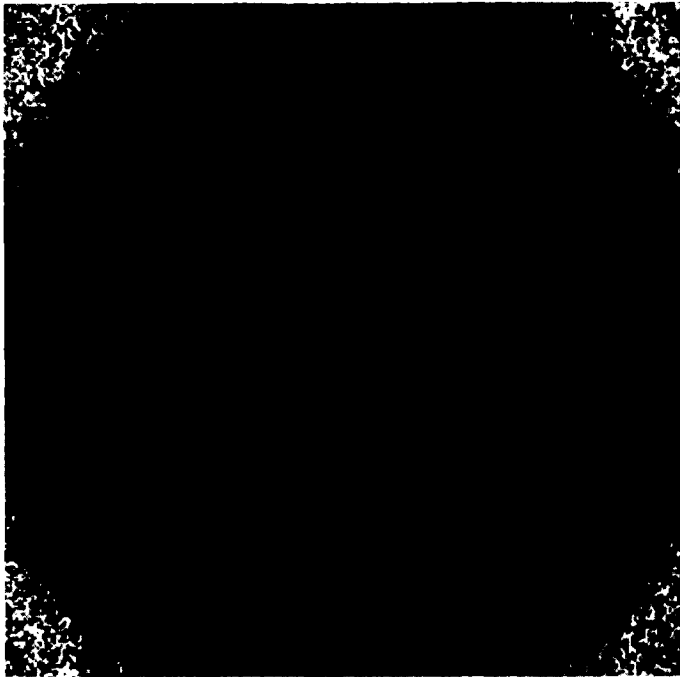


2a

Figs. 1a, 2a.



1b

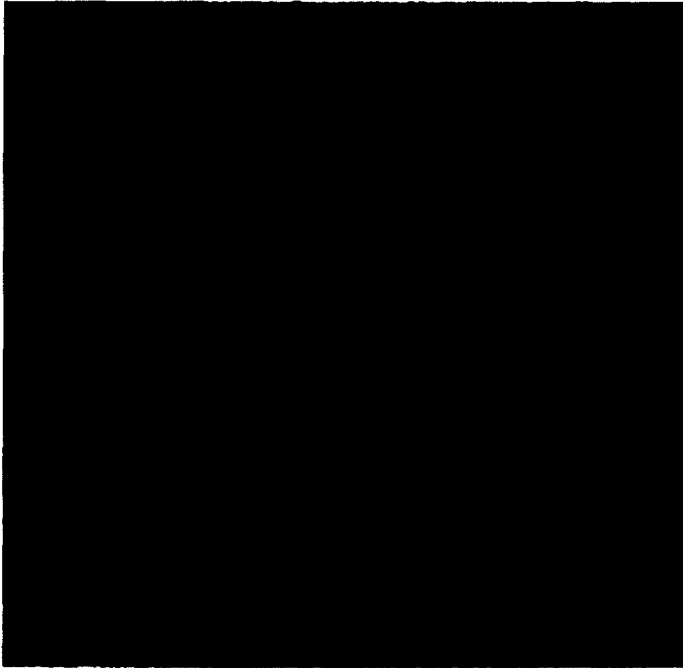


2b

Figs. 1b, 2b.



1c



2c

Figs. 1c, 2c.

The full details of the parameter estimation scheme (called the ‘‘Monte Carlo differential rotation’’ technique) are given in ref. [10]; in outline a quadratic error function is defined and the parameters are adjusted for best fit. The only complication is that while it is easy to compute  $k_\lambda$  given  $G$ ,  $\lambda$ ,  $k_1$  (by applying  $T_\lambda$ ), the inverse (finding  $\lambda$  given  $k_\lambda$ ,  $k_1$ ,  $G$ ) involves solving a transcendental equation and is numerically prohibitive due to the large number of times it must be solved by the regression algorithm. The error in the parameters is therefore only statistically estimated using a Monte Carlo method (hence the name).

The resulting parameters are shown in table I, the corresponding ‘‘balls’’ are superposed in fig. 2, showing the fairly accurate fits that are achieved. We may note the following:

(a) It has been found [12] (using isotropic spectra) that the parameter  $s$  is mostly a function of wavelength of the radiation; this is confirmed here.

(b) In the two cases where sphero-scales exist, they are right in the middle of the ‘‘meso-scale’’, the horizontal scale corresponding to the exponential fall-off height for the pressure field ( $\approx 10$  km). This is totally at odds with the standard view which postulates a qualitative change (‘‘dimensional transition’’),

Table I

A comparison of the characteristics of the three satellite images discussed in the text.  $a$  (see eq. (3)) was found to be real in all cases, the total rotation between small and large scale structures is therefore bounded,  $|\Delta\theta|_{\max}$  providing an estimate of this bound.

|                         | Image 1                         | Image 2                   | Image 3                      |
|-------------------------|---------------------------------|---------------------------|------------------------------|
| Image type              | Infra red, marine stratocumulus | Visible, stratocumulus    | Visible, midlatitude cyclone |
| Range of scales         | $1.1 \times 256 = 281$ km       | $1.1 \times 512 = 563$ km | $2.2 \times 512 = 1126$ km   |
| $s$                     | $2.5 \pm 0.1$                   | $2.18 \pm 0.05$           | $2.10 \pm 0.01$              |
| Sphero-scale            | $3.5 \pm 0.8$ km                | $3.9 \pm 0.6$ km          | not applicable <sup>a)</sup> |
| $c$                     | $-0.43 \pm 0.08$                | $-0.32 \pm 0.05$          | $-0.18 \pm 0.03$             |
| $f$                     | $0.0 \pm 0.1$                   | $-0.01 \pm 0.02$          | $0.00 \pm 0.02$              |
| $e$                     | $-0.4 \pm 0.2$                  | $0.17 \pm 0.04$           | $0.04 \pm 0.05$              |
| $a$                     | $0.2 \pm 0.3$                   | $0.28 \pm 0.07$           | $0.18 \pm 0.03$              |
| $ \Delta\theta _{\max}$ | $60 \pm 30^\circ$               | $30 \pm 10^\circ$         | $10 \pm 10^\circ$            |

<sup>a)</sup>As indicated in the text, no spheroscale is apparent in this case, using eq. (4), in units of pixels in wavenumber space (fig. 2c), choosing an energy density level arbitrarily, near the centre of fig. 2c, we found  $r_0 = 108 \pm 1$ ,  $a_1 = -20 \pm 1$ ,  $b_1 = -23 \pm 1$ ,  $a_2 = 17 \pm 1$ ,  $b_2 = -6 \pm 1$ .

Fig. 1. (a, b, c) A grey shade rendition of images 1, 2, 3, the radiance fields studied in the text, see table I for details.

Fig. 2. (a, b, c) A grey shade rendition of the log of the Fourier space energy density of images 1, 2, 3. Superposed are the isolines as deduced from the Monte Carlo differential rotation technique using the parameters in table I.

“meso-scale gap”) in the meso-scale; this may be the primary way that the vertical scale height influences the horizontal structure.

(c) The primary variation in the scaling parameters seems to be  $c$ ,  $e$ , which vary much more than  $a$  (which is always positive indicating stratification dominance). This suggests that  $a$  is a more fundamental parameter.

(d) The cases with the most rotation of structures with scales are the “texture” fields 1, 2. This is not as surprising as it may seem; computer simulations of fractal clouds show that the anisotropy is indeed associated with texture [13]; whereas the cyclone is already nearly a (self-similar, isotropic) scale invariant log-spiral.

Obviously many more pictures must be analysed before more definite conclusions can be reached<sup>#5</sup>. The statistics of the parameters should be examined, higher order moments should be studied, and finally multifractal simulations [14] should be performed to confirm that the analyzed generator does indeed correspond to the true generator.

## References

- [1] B.B. Mandelbrot, *The Fractal Geometry of Nature* (Freeman, San Francisco, 1983) pp. 452.
- [2] D. Schertzer and S. Lovejoy, in: *Proc. 4th Symp. on Turbulent Shear Flows*, secs. 11.1–11.8, Karlsruhe, West Germany, 1983; *Turbulent Shear Flow*, vol. 4, B. Launder, ed. (Springer, 1985) pp. 7–33.
- [3] D. Schertzer and S. Lovejoy, *Pageoph.* 130 (1989) 57.
- [4] B. Carter and R.N. Henrickson, *J. Math. Phys.* 32 (1992) 2580.
- [5] D. Schertzer and S. Lovejoy, *Phys. Chem. Hydrodyn. J.* 6 (1985) 623; *Ann. Math. Que.* 11 (1987) 139; *J. Geophys. Res.* 92 (1987) 9692.
- [6] D. Schertzer and S. Lovejoy, in: *Fractals: Their Physical Origins and Properties*, L. Pietronero, ed. (Plenum, New York, 1989) pp. 49–79.
- [7] D. Schertzer and S. Lovejoy, in: *Scaling, Fractals and Non-Linear Variability in Geophysics*, D. Schertzer and S. Lovejoy, eds. (Kluwer, Dordrecht, 1991) pp. 41–82.
- [8] S. Lovejoy, D. Schertzer and A.A. Tsonis, *Science* 235 (1987) 1036.
- [9] S. Lovejoy and D. Schertzer, in: *Scaling, Fractals and Non-Linear Variability in Geophysics*, D. Schertzer and S. Lovejoy, eds. (Kluwer, Dordrecht, 1991) pp. 111–144.
- [10] K. Pflug, MSc. Thesis, Physics Dept., McGill Univ., (1991) 94 pp; K. Pflug, S. Lovejoy and D. Schertzer, in: *Nonlinear Dynamics of Structures*, R.Z. Sagdeev et al., eds. (World Scientific, Singapore, 1991) pp. 71–80.
- [11] P. Gabriel, S. Lovejoy, D. Schertzer and G.L. Austin, *Geophys. Res. Lett.* 15 (1988) 1373; S. Lovejoy and D. Schertzer, *J. Geophys. Res.* 95 (1990) 2021.
- [12] Y. Tessier, S. Lovejoy and D. Schertzer, *J. Appl. Meteor.*, submitted; S. Lovejoy, D. Schertzer, P. Silas, Y. Jessier and D. Lavallée, *Ann. Geophys.*, submitted.
- [13] S. Lovejoy and D. Schertzer, *Water Resour. Res.* 21 (1985) 1233.
- [14] J. Wilson, S. Lovejoy and D. Schertzer, in: *Scaling, Fractals and Non-Linear Variability In Geophysics*, D. Schertzer and S. Lovejoy, eds. (Kluwer, Dordrecht, 1991) pp. 185–208.

<sup>#5</sup> Six other cases have already been analyzed in less detail; they show qualitatively the same behavior.